PHYSICAL REVIEW B **94**, 060506(R) (2016)

Observation of Ising spin-nematic order and its close relationship to the superconductivity in FeSe single crystals

Dongna Yuan,[1] Jie Yuan,[1] Yulong Huang,[1] Shunli Ni,[1] Zhongpei Feng,[1] Huaxue Zhou,[1] Yiyuan Mao,[1] Kui Jin,[1,2] Guangming Zhang,[3] Xiaoli Dong,[1,2,*] Fang Zhou,[1,2,†] and Zhongxian Zhao[1,2]

[1]*Beijing National Laboratory for Condensed Matter Physics, Institute of Physics, Chinese Academy of Science, Beijing 100190, China*

[2]*University of Chinese Academy of Sciences, Beijing 100049, China*

[3]*State Key Laboratory of Low Dimensional Quantum Physics and Department of Physics, Tsinghua University, Beijing 100084, China*

(Received 2 May 2016; revised manuscript received 1 August 2016; published 18 August 2016)

Superconducting FeSe single crystals of (001) orientation are synthesized via a hydrothermal ion-release route. An Ising spin-nematic order is identified by our systematic measurements of in-plane angular-dependent magnetoresistance (AMR) and static magnetization. The turn-on temperature of anisotropic AMR signifies the Ising spin-nematic ordering temperature T_{sn}, below which a twofold rotational symmetry is observed in the iron plane. A downward curvature appears below T_{sn} in the temperature dependence of static magnetization for the weak in-plane magnetic field as reported previously. Remarkably, we find a universal linear relationship between T_{c} and T_{sn} among various superconducting samples, indicating that the spin nematicity and the superconductivity in FeSe have a common microscopic origin.

DOI: 10.1103/PhysRevB.94.060506

The tetragonal β-FeSe was reported to show bulk superconducting transition at $T_{\mathrm{c}} \sim 8$ K [1,2]. It is notable that its T_{c} can be enhanced to 36.7 K under high pressure [3–6] and even to $\sim$48 K via charge injection [7]. Also, a higher T_{c} than the binary FeSe is always achieved in ion/cluster intercalated iron selenides. For example, the superconductivity with $T_{\mathrm{c}} \sim 42$ K has been realized in $(\mathrm{Li}_{1-x}\mathrm{Fe}_x)\mathrm{OHFe}_{1-y}\mathrm{Se}$ [8], where the two dimensionality of the electronic structure of the iron plane is enhanced due to the expansion in the interlayer separation [9,10]. In contrast, the bulk FeSe displays the maximum interlayer compactness in the iron-based superconductors and thus the lowest T_{c}.

In FeSe superconductors, no antiferromagnetic long-range order was reported to exist in ambient pressure, but the presence of the rotational symmetry breaking in the electronic structure of the iron plane and its implication for superconducting pairing have drawn much attention [11–17]. It has been argued that the tetragonal-to-orthorhombic structure transition at $T_{\mathrm{s}} \sim 90$ K is driven by the ferro-orbital ordering with unequal occupancies of the $3d_{xz}/3d_{yz}$ orbitals [18,19]. However, the structural transition temperature T_{s} remains nearly the same for various samples showing different T_{c}'s (see below in Fig. 4). Recent neutron scattering measurements [20–22] suggest that the electron pairing for the superconductivity is closely related to the stripelike $(\pi,0)$ antiferromagnetic (AFM) spin fluctuations and a sharp spin resonance is observed in the superconducting phase. Therefore, the key issue turns out to be whether any peculiar order of the spin origin showing the rotational symmetry breaking exists and how it is related to the superconductivity in FeSe.

Here we report the presence of an Ising spin-nematic order in our FeSe single crystal samples based on the measurements of angular-dependent magnetoresistance (AMR) and static magnetization. The onset temperature T_{sn} of this nematic order strongly depends on the superconducting transition temperature (T_{c}), and spans a wide range from far below to beyond the structural transition temperature (T_{s}). Our results suggest that the spin nematicity is driven by strongly frustrated spins with the $(\pi,0)$ stripe fluctuations predominating in bulk FeSe. Importantly, a universal linear relationship between T_{c} and T_{sn} is found among various superconducting samples, indicating that the spin nematicity and the superconductivity in FeSe have a common microscopic origin.

In order to identify the electronic correlations in the iron plane crucial for the superconductivity, sizable FeSe crystal samples of (001) plane orientation with different T_{c}'s are essential. Although the samples of the (001) orientation can be obtained by, e.g., vapor transport growth, it is a very time-consuming process. On the other hand, the high-temperature growth by flux-free floating-zone or flux method only produces the samples with (101) orientation. Most recently, by a high-efficient hydrothermal ion-release/introduction technique, we have successfully synthesized large FeSe single crystal samples of the (001) orientation. The details of sample preparation have been reported in Ref. [23], similar to the ion/cluster exchange growth of large $(\mathrm{Li}_{0.84}\mathrm{Fe}_{0.16})\mathrm{OHFe}_{0.98}\mathrm{Se}$ single crystals [10]. Via this hydrothermal process, the superconducting FeSe single crystal can be derived from the insulating $\mathrm{K}_{0.8}\mathrm{Fe}_{1.6}\mathrm{Se}_2$ matrix. Namely, the interlayer K ions in the matrix are completely *released* and the $\sqrt{5}\times\sqrt{5}$ ordered vacant Fe sites $\sim$20% in amount in the $\mathrm{Fe}_{0.8}\mathrm{Se}$ layers are occupied by *introduced* Fe ions. The end FeSe single crystal naturally inherits the original (001) orientation of the matrix, in which no trace of K is detected by energy-dispersive x ray. Powder x-ray diffraction confirms the pure tetragonal β-FeSe phase with the lattice parameters $a = 3.7725(1)$ Å and $c = 5.5247(2)$ Å for the sample of $T_{\mathrm{c}} \sim 7.6$ K [23]. The magnetic measurements were conducted on a Quantum Design MPMS-XL1 system of a small remnant field 4 mOe. The

*dong@iphy.ac.cn

†fzhou@iphy.ac.cn

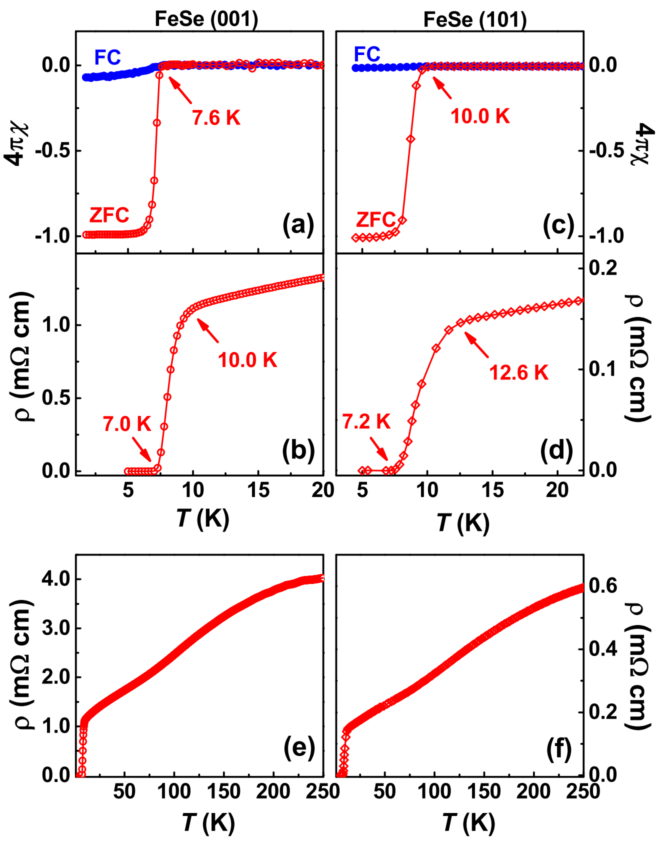

FIG. 1. Temperature dependences of the static magnetic susceptibility, corrected for demagnetization factor, and the electrical resistivity for the two typical FeSe single crystal samples with (001) and (101) orientations. (a) and (c) The data of magnetic susceptibility; (b) and (d) the electrical resistivity near the superconducting transitions; (e) and (f) the resistivity up to 250 K. The magnetic measurements are performed under $H = 1$ Oe.

electrical resistivity and the angular-dependent magnetoresistance were measured on a Quantum Design PPMS-9.

For a typical hydrothermal crystal sample displaying the (001) orientation, the bulk superconductivity at $T_c \sim 7.6$ K is confirmed by the magnetic and electrical resistivity measurements, shown in Figs. 1(a) and 1(b). The high superconducting quality is demonstrated by the sharp diamagnetic transitions as well as the 100% diamagnetic shielding, although the sample shows a crystal mosaic of approximately 5° in terms of the full width at half maximum of x-ray rocking curve [23]. In this work, we also performed similar measurements on a flux-grown FeSe crystal sample of (101) orientation exhibiting a higher T_c [24]. Its superconductivity is shown in Figs. 1(c) and 1(d). The temperature dependences of the normal state resistivity in the whole measuring temperature range for the two typical samples are displayed in Figs. 1(e) and 1(f), respectively. All the T_c values here are determined by the onset temperatures of the diamagnetic transition, defined as that where the shielding and Meissner signals clearly separate from one another. We find that the T_c value of FeSe is sensitive to the carrier concentrations of electron and hole bands from our Hall measurements (to be reported elsewhere).

With our single crystal samples, the angular-dependent magnetoresistance measurements are performed. We fixed the

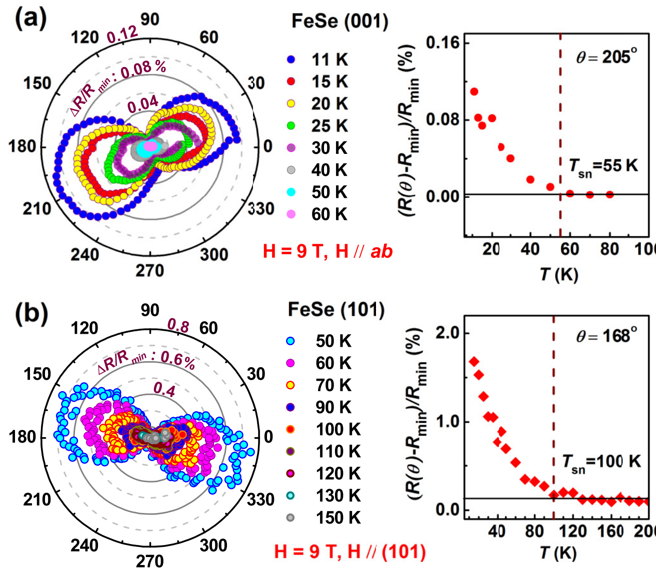

FIG. 2. Temperature dependences of the angular-dependent magnetoresistance showing the twofold rotational symmetry below ~55 K (the upper right) and ~100 K (the lower right). (a) The FeSe crystal sample of (001) orientation with $T_c \sim 7.6$ K. (b) the sample of (101) orientation with $T_c \sim 10.0$ K. The θ is the angle between the directions of the external field (H) and the current (I), with $\theta = 0°$ corresponding to $H \perp I$.

current direction and varied the angle (θ) between the directions of the external field (H) and the current (I), with $\theta = 0°$ corresponding to $H \perp I$. Remarkably, for both the FeSe crystal samples with the lower $T_c \sim 7.6$ K and the higher $T_c \sim 10.0$ K, the AMR in the normal state exhibits a *twofold* rotational symmetry, which is turned on below $T_{sn} \sim 55$ K and ~100 K as shown in Figs. 2(a) and 2(b), respectively. The anisotropy in AMR becomes enhanced with decreasing temperature. Such an enhancement in charge scatterings is also manifested in temperature-dependent magnetoresistance (MR) [25]. Our observation of the AMR anisotropy with the twofold rotational symmetry thus provides decisive evidence for the presence of a nematic ordering different from the ferro-orbital ordering, which is accompanied with the structural transition occurring at almost the same temperature ($T_s \sim 90$ K) in samples with different T_c's.

Furthermore, a downward curvature below $T_{sn} \sim 55$ K for the (001) crystal sample of $T_c \sim 7.6$ K has been observed in the static magnetization under an in-plane magnetic field of 0.1 T (Fig. 5a in Ref. [23]). Such a feature is strongly dependent on the magnitude of the magnetic field: it fades out when the field is lowered to 0.01 T (Fig. 5b in Ref. [23]). This indicates that the strong quantum spin frustrations predominate in the iron plane. Although the orbital ordering below T_s is of the twofold rotational symmetry, the obvious downward feature of in-plane static magnetization below the characteristic $T_{sn} \sim 55$ K, which is far below T_s, suggests that the twofold anisotropy identified by our AMR measurements is closely related to the frustrated spins with the anisotropic magnetic fluctuations, rather than the orbital ordering. Therefore, we are led to the conclusion that an Ising-like spin-nematic order emerges below T_{sn}. The corresponding order parameter is characterized by

$$\sigma = \langle S_i S_{i+x} - S_i S_{i+y} \rangle, \tag{1}$$

where S_{i+x} and S_{i+y} stand for the nearest-neighbor spins of the spin S_i on the square lattice, respectively. Actually, such Ising spin nematicity is argued to exist in the strongly frustrated limit of the quantum frustrated spin-1 Heisenberg model with nearest-neighbor antiferromagnetic coupling and next-nearest-neighbor antiferromagnetic coupling [12,16,26–29]. Consequently, the appearance of the twofold anisotropy in AMR for the (001) sample is well explicable by the temperature-dependent anisotropic scattering of the charge carriers caused by the spin-nematic order below T_{sn}. For the AMR measurement on the sample of (101) orientation, the iron plane component of the magnetic field takes effect. Considering the $(\pi,0)$ stripe spin fluctuations reported for FeSe superconductors, we argue that the maxima of the anisotropic AMR points in the crystallographic *a* direction with antiferromagnetic correlations and the minima in the *b* direction with ferromagnetic correlations.

Moreover, we have also hydrothermally synthesized another FeSe single crystal of (001) orientation, and its characteristic temperatures are determined as $T_c \sim 6.8$ K and $T_{sn} \sim 37.5$ K, shown in Fig. 3. The difference in T_c value results from the difference in concentrations of electron and hole bands on the basis of our Hall resistance measurements (to be reported elsewhere). When summarizing all the data of our three single crystal samples, we found a remarkable linear relationship between T_c and T_{sn} (the dotted straight line in Fig. 4). The fitting gives rise to an expression

$$T_c = \alpha T_{sn} + T_{min}, \tag{2}$$

with $\alpha \sim 0.052$ and $T_{min} \sim 4.8$ K. Moreover, we also collect three other sets of T_c and T_{sn} given by either the onset temperature of MR or the cusp temperature of the in-plane magnetic magnetization on FeSe single crystal samples of the (001) orientation [25,30,31]. All the collected T_c and T_{sn} well satisfy this linear relationship as well. Meanwhile, the structural transition temperatures (T_s's) by the x-ray or neutron diffractions on various FeSe samples with different T_c's available from the literature [19,20,22,32–36] are plotted in Fig. 4. In contrast to the T_s remaining at nearly the same value of $\sim$90 K, the value of the spin-nematic ordering temperature T_{sn} varies with T_c in a wide range from far below to beyond T_s. Therefore, the superconductivity and the spin nematicity are correlated by the stripe AFM spin fluctuations, rather than the structural phase transition or the orbital ordering. Interestingly, this universal linear relationship allows the spin-nematic ordering to coincide with the superconducting transition at $T_{min}/(1-\alpha) \sim 5.1$ K, which is worthy of a further study.

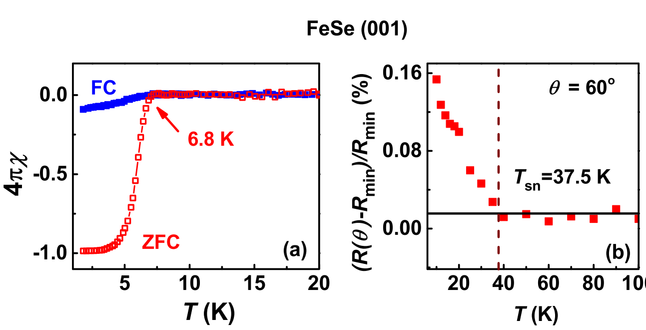

FIG. 3. (a) Temperature dependence of the static magnetic susceptibility for the hydrothermal FeSe crystal sample of (001) orientation with the $T_c \sim 6.8$ K. (b) Its temperature dependence of the maxima in anisotropic AMR showing the $T_{sn} \sim 37.5$ K. The θ is the angle between the directions of the external field (H) and the current (I), with $\theta = 0^\circ$ corresponding to $H \perp I$.

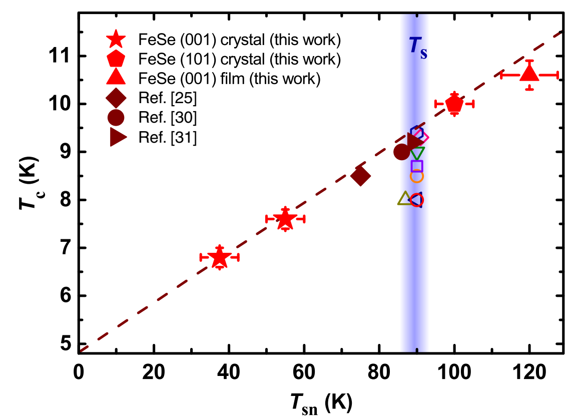

FIG. 4. The universal linear relationship between the superconducting transition temperature (T_c) and the Ising spin-nematic ordering temperature (T_{sn}) among various FeSe samples (the solid symbols). The hollow symbols in the vertical blue-shaded area represent the structure phase transition temperatures (T_s's) by the x-ray or neutron diffractions on various FeSe samples of different T_c's [19,20,22,32–36]. The experimental uncertainty for the T_c values of our crystal samples, defined as the temperatures where the shielding and Meissner signals clearly separate from one another, is estimated as ± 0.25 K from the signal responses. The T_{sn}'s have an estimated error $< \pm 5$ K, which is the temperature sampling interval.

It needs to be emphasized that, for the FeSe samples with T_c's around 9.5 K, both the spin nematicity transition and the ferro-orbital ordering/structure transition happen to occur in the vicinity of $\sim$90 K, as shown in Fig. 4. So it is very difficult to distinguish experimentally these different ordering transitions in such samples. However, our specific samples cover the T_c values from 6.8 to 10.6 K, so that the spin-nematic ordering temperature spans from 37.5 to 120 K, well separated from the structural transition temperature $\sim$90 K. Therefore, our results have disentangled the essential role played by the spin-nematic ordering in the superconducting pairing, resolving a long-standing puzzle in bulk FeSe superconductors.

In conclusion, we have experimentally evidenced the emergence of the spin-nematic ordering below T_{sn} in the normal state of the superconducting FeSe single crystals. The universal linear relationship between T_c and T_{sn} has been found, which spans a wide temperature range. Our results have shed new light on the mechanism of unconventional superconductivity in FeSe, including its drastic enhancement of the superconducting transition temperature under pressure when the nematicity is suppressed.

Note added. We find that the T_c ($\sim$10.6 K) and T_{sn} ($\sim$120 K) of our FeSe film, newly prepared by pulsed laser deposition [37], also follow the universal linear relationship found in this work.

This work is supported by National Natural Science Foundation of China (Projects 11574370 and 11190020), the National Basic Research Program of China (Projects 2013CB921700 and 2016YFA0300301), and "Strategic Priority Research Program (B)" of the Chinese Academy of Sciences (Grant No. XDB07020100). X.L.D., F.Z., and Z.X.Z. planned and designed the Project and summarized the data. D.N.Y., S.L.N., and Y.L.H. contributed to single crystal synthesis. Z.P.F. contributed to film growth. J.Y., D.N.Y., and Y.L.H. measured transport and magnetic data analyzed by K.J., J.Y., and X.L.D. with theoretical support from G.M.Z. G.M.Z. introduced the theoretical model. F.Z., X.L.D., and G.M.Z. wrote the paper. All authors provided comments for the paper.

[1] F. C. Hsu, J. Y. Luo, K. W. Yeh, T. K. Chen, T. W. Huang, P. M. Wu, Y. C. Lee, Y. L. Huang, Y. Y. Chu, D. C. Yan, and M. K. Wu, Proc. Natl. Acad. Sci. USA **105**, 14262 (2008).

[2] T. M. McQueen, Q. Huang, V. Ksenofontov, C. Felser, Q. Xu, H. Zandbergen, Y. S. Hor, J. Allred, A. J. Williams, D. Qu, J. Checkelsky, N. P. Ong, and R. J. Cava, Phys. Rev. B **79**, 014522 (2009).

[3] S. Medvedev, T. M. McQueen, I. A. Troyan, T. Palasyuk, M. I. Eremets, R. J. Cava, S. Naghavi, F. Casper, V. Ksenofontov, G. Wortmann, and C. Felser, Nat. Mater. **8**, 630 (2009).

[4] M. Bendele, A. Amato, K. Conder, M. Elender, H. Keller, H. H. Klauss, H. Luetkens, E. Pomjakushina, A. Raselli, and R. Khasanov, Phys. Rev. Lett. **104**, 087003 (2010).

[5] J. P. Sun, K. Matsuura, G. Z. Ye, Y. Mizukami, M. Shimozawa, K. Matsubayashi, M. Yamashita, T. Watashige, S. Kasahara, Y. Matsuda, J.-Q. Yan, B. C. Sales, Y. Uwatoko, J.-G. Cheng, and T. Shibauchi, Nat. Commun. **7**, 12146 (2016).

[6] T. Terashima, N. Kikugawa, S. Kasahara, T. Watashige, Y. Matsuda, T. Shibauchi, and S. Uji, Phys. Rev. B **93**, 180503(R) (2016).

[7] B. Lei, J. H. Cui, Z. J. Xiang, C. Shang, N. Z. Wang, G. J. Ye, X. G. Luo, T. Wu, Z. Sun, and X. H. Chen, Phys. Rev. Lett. **116**, 077002 (2016).

[8] X. F. Lu, N. Z. Wang, H. Wu, Y. P. Wu, D. Zhao, X. Z. Zeng, X. G. Luo, T. Wu, W. Bao, G. H. Zhang, F. Q. Huang, Q. Z. Huang, and X. H. Chen, Nat. Mater. **14**, 325 (2015).

[9] X. Dong, H. Zhou, H. Yang, J. Yuan, K. Jin, F. Zhou, D. Yuan, L. Wei, J. Li, X. Wang, G. Zhang, and Z. Zhao, J. Am. Chem. Soc. **137**, 66 (2015).

[10] X. Dong, K. Jin, D. Yuan, H. Zhou, J. Yuan, Y. Huang, W. Hua, J. Sun, P. Zheng, W. Hu, Y. Mao, M. Ma, G. Zhang, F. Zhou, and Z. Zhao, Phys. Rev. B **92**, 064515 (2015).

[11] A. E. Böhmer and C. Meingast, Compt. Rend. Phys. **17**, 90 (2016).

[12] J. K. Glasbrenner, I. I. Mazin, H. O. Jeschke, P. J. Hirschfeld, R. M. Fernandes, and R. Valenti, Nat. Phys. **11**, 953 (2015).

[13] A. V. Chubukov, R. M. Fernandes, and J. Schmalian, Phys. Rev. B **91**, 201105 (2015).

[14] M. A. Tanatar, A. E. Böhmer, E. I. Timmons, M. Schütt, G. Drachuck, V. Taufour, S. L. Bud'ko, P. C. Canfield, R. M. Fernandes, and R. Prozorov, arXiv:1511.04757.

[15] Y. Hu, X. Ren, R. Zhang, H. Luo, S. Kasahara, T. Watashige, T. Shibauchi, P. Dai, Y. Zhang, Y. Matsuda, and Y. Li, Phys. Rev. B **93**, 060504 (2016).

[16] A. V. Chubukov, M. Khodas, and R. M. Fernandes, arXiv:1602.05503.

[17] M. Abdel-Hafiez, Y. J. Pu, J. Brisbois, R. Peng, D. L. Feng, D. A. Chareev, A. V. Silhanek, C. Krellner, A. N. Vasiliev, and X.-J. Chen, Phys. Rev. B **93**, 224508 (2016).

[18] T. Shimojima, Y. Suzuki, T. Sonobe, A. Nakamura, M. Sakano, J. Omachi, K. Yoshioka, M. Kuwata-Gonokami, K. Ono, H. Kumigashira, A. E. Böhmer, F. Hardy, T. Wolf, C. Meingast, H. v. Löhneysen, H. Ikeda, and K. Ishizaka, Phys. Rev. B **90**, 121111 (2014).

[19] S. H. Baek, D. V. Efremov, J. M. Ok, J. S. Kim, J. van den Brink, and B. Buchner, Nat. Mater. **14**, 210 (2015).

[20] M. C. Rahn, R. A. Ewings, S. J. Sedlmaier, S. J. Clarke, and A. T. Boothroyd, Phys. Rev. B **91**, 180501 (2015).

[21] Q. Wang, Y. Shen, B. Pan, X. Zhang, K. Ikeuchi, K. Iida, A. D. Christianson, H. C. Walker, D. T. Adroja, M. Abdel-Hafiez, X. Chen, D. A. Chareev, A. N. Vasiliev, and J. Zhao, Nat. Commun. **7**, 12182 (2016).

[22] Q. Wang, Y. Shen, B. Pan, Y. Hao, M. Ma, F. Zhou, P. Steffens, K. Schmalzl, T. R. Forrest, M. Abdel-Hafiez, X. Chen, D. A. Chareev, A. N. Vasiliev, P. Bourges, Y. Sidis, H. Cao, and J. Zhao, Nat. Mater. **15**, 159 (2016).

[23] D. Yuan, Y. Huang, S. Ni, H. Zhou, Y. Mao, W. Hu, J. Yuan, K. Jin, G. Zhang, X. Dong, and F. Zhou, Chin. Phys. B **25**, 077404 (2016).

[24] M. W. Ma, D. N. Yuan, Y. Wu, X. L. Dong, and F. Zhou, Phys. C (Amsterdam, Neth.) **506**, 154 (2014).

[25] S. Rößler, C. Koz, L. Jiao, U. K. Rößler, F. Steglich, U. Schwarz, and S. Wirth, Phys. Rev. B **92**, 060505 (2015).

[26] C. Fang, H. Yao, W.-F. Tsai, J. P. Hu, and S. A. Kivelson, Phys. Rev. B **77**, 224509 (2008).

[27] C. K. Xu and S. Sachdev, Nat. Phys. **4**, 898 (2008).

[28] F. Wang, S. A. Kivelson, and D.-H. Lee, Nat. Phys. **11**, 959 (2015).

[29] R. Yu and Q. Si, Phys. Rev. Lett. **115**, 116401 (2015).

[30] Y. Sun, S. Pyon, and T. Tamegai, Phys. Rev. B **93**, 104502 (2016).

[31] T. Urata, Y. Tanabe, K. K. Huynh, Y. Yamakawa, H. Kontani, and K. Tanigaki, Phys. Rev. B **93**, 014507 (2016).

[32] T. M. McQueen, A. J. Williams, P. W. Stephens, J. Tao, Y. Zhu, V. Ksenofontov, F. Casper, C. Felser, and R. J. Cava, Phys. Rev. Lett. **103**, 057002 (2009).

[33] A. E. Böhmer, F. Hardy, F. Eilers, D. Ernst, P. Adelmann, P. Schweiss, T. Wolf, and C. Meingast, Phys. Rev. B **87**, 180505 (2013).

[34] C. Koz, M. Schmidt, H. Borrmann, U. Burkhardt, S. Rößler, W. Carrillo-Cabrera, W. Schnelle, U. Schwarz, and Y. Grin, Z. Anorg. Allg. Chem. **640**, 1600 (2014).

[35] K. Kothapalli, A. E. Böhmer, W. T. Jayasekara, B. G. Ueland, P. Das, A. Sapkota, V. Taufour, Y. Xiao, E. E. Alp, S. L. Bud'ko, P. C. Canfield, A. Kreyssig, and A. I. Goldman, arXiv:1603.04135.

[36] U. Pachmayr, N. Fehn, and D. Johrendt, Chem. Commun. **52**, 194 (2016).

[37] Z. Feng, J. Yuan, and K. Jin (unpublished).